Thermal decomposition of toluene: Overall rate and branching ratio

ARTICLE *in* PROCEEDINGS OF THE COMBUSTION INSTITUTE · JANUARY 2007

Impact Factor: 2.26 · DOI: 10.1016/j.proci.2006.07.002

3 AUTHORS, INCLUDING:

Matthew A. Oehlschlaeger
Rensselaer Polytechnic Institute
75 PUBLICATIONS **1,607** CITATIONS

Available online at www.sciencedirect.com
ScienceDirect
Proceedings of the Combustion Institute 31 (2007) 211–219
Proceedings of the Combustion Institute
www.elsevier.com/locate/proci

Thermal decomposition of toluene: Overall rate and branching ratio

Matthew A. Oehlschlaeger [1], David F. Davidson *, Ronald K. Hanson

High Temperature Gasdynamics Laboratory, Department of Mechanical Engineering, Stanford University, Stanford, CA 94305-3032, USA

Abstract

The two-channel thermal decomposition of toluene, $C_6H_5CH_3 \rightarrow C_6H_5CH_2 + H$ (1) and $C_6H_5CH_3 \rightarrow C_6H_5 + CH_3$ (2), was investigated in shock tube experiments over the temperature range of 1400–1780 K at a pressure of 1.5 (±0.1) bar. Rate coefficients for reactions (1) and (2) were determined by monitoring benzyl radical ($C_6H_5CH_2$) absorption at 266 nm during the decomposition of toluene diluted in argon and modeling the temporal behavior of the benzyl concentration with a kinetic model. The first-order rate coefficients determined at a pressure of 1.5 bar are expressed by $k_1(T) = 2.09 \times 10^{15} \exp(-87510\ [\text{cal/mol}]/RT)\ [\text{s}^{-1}]$ and $k_2(T) = 2.66 \times 10^{16} \exp(-97880\ [\text{cal/mol}]/RT)\ [\text{s}^{-1}]$. The resulting branching ratio, $k_1/(k_1 + k_2)$, ranges from 0.8 at 1350 K to 0.6 at 1800 K.

Keywords: Shock tube; Toluene; Decomposition; Pyrolysis

1. Introduction

In the past several years there has been considerable interest in developing detailed kinetic mechanisms to describe the combustion of aromatic fuels [1–6]. Although detailed mechanisms exist for aromatic combustion, there is a lack of high-quality rate coefficient data for many of the reactions of importance. One class of reactions of importance in these mechanisms is the thermal decomposition of aromatics.

For example, the decomposition of toluene is an important initiation step in the oxidation of toluene at moderate- to high-temperatures (>1200 K). Despite its importance the decomposition of toluene is not well understood due to complications in its measurement. The primary complication is that toluene decomposition takes place via two channels

$$C_6H_5CH_3 \rightarrow C_6H_5CH_2 + H \quad (1)$$

$$C_6H_5CH_3 \rightarrow C_6H_5 + CH_3 \quad (2)$$

making isolated measurement of the two rate coefficients, k_1 and k_2, difficult. Additionally, fast secondary and recombination reactions occur in parallel with the decomposition, further complicating kinetic isolation of reactions (1) and (2).

Previous measurements of toluene decomposition have been made at high temperatures behind shock waves using time-of-flight mass spectrometry [7], laser-schlieren [7], ultraviolet absorption [8–13], and H-atom ARAS [14–16]. Additionally, laser-excitation techniques used to measure

* Corresponding author. Fax: +1 650 723 1748.
E-mail address: dfd@stanford.edu (D.F. Davidson).
[1] Present address: Department of Mechanical, Aerospace, and Nuclear Engineering, Rensselaer Polytechnic Institute, Troy, NY, USA.

1540-7489/$ - see front matter
doi:10.1016/j.proci.2006.07.002

energy-specific rate coefficients for toluene decomposition have been performed [17,18]. Astholz et al. [10,11] first investigated the shock-initiated thermal decomposition of toluene using lamp absorption in the ultraviolet to observe benzyl radicals. However, these early studies proved difficult due to a lack of understanding of the complexity of secondary chemistry. As an understanding of the secondary chemistry was developed, further studies were performed using ultraviolet lamp absorption of benzyl by Müller-Markgraf and Troe [9,12], Brouwer et al. [13], and Hippler et al. [8] identifying reaction (1) as the dominate reaction. Pamidimukkala et al. [7] performed laser-schlieren densitometry and time-of-flight mass spectrometry measurements in shock-heated gas mixtures of high-concentrations of toluene (0.5–4%) in krypton and neon. They concluded that the phenyl channel, reaction (2), dominated at high-temperatures (1550–2200 K) due to the fast equilibration of reactions (1) and (−1) and the expected large *A*-factor for reaction (2). H-atom ARAS measurements in shock-heated gases have been made by Braun-Unkhoff et al. [15], Rao and Skinner [16], and most recently Eng et al. [14] for rate determinations of reaction (1). Eng et al. [14] also performed master equation calculations to predict the temperature- and pressure-dependence of the branching ratio, $k_1/(k_1+k_2)$. In addition to shock tube measurements, laser-excitation measurements have been performed by Brand et al. [17] and Luther et al. [18] to determine energy-specific rate coefficients for the thermal decomposition of toluene. Luther et al. [18] also used multiphoton ionization to determine CH_3 yields and therefore deduce branching ratios.

The measurements presented here utilize laser absorption of benzyl radicals in shock-heated toluene/argon mixtures. The use of laser absorption provides significantly increased signal-to-noise (approximately a factor of 10) compared to previous measurements of benzyl made using less spectrally intense lamp sources [8–13]; consequently, the resulting rate coefficient determinations show less scatter and are less uncertain. In comparison to the previous H-atom ARAS measurements, the experiments reported here have been performed at higher concentrations (approximately a factor of 10) required by the smaller absorption cross-section of benzyl at 266 nm in comparison to the Lyman-α 121.6 nm H-atom absorption cross-section. Therefore, the current measurements exhibit greater sensitivity to secondary chemistry than the previous H-atom ARAS measurements. However, the current results provide significantly greater *absorbance* ($-\ln(I/I_0)$) signal-to-noise than the ARAS measurements and therefore the resulting rate coefficients show significantly less scatter and similar uncertainty when compared with the previous H-atom ARAS measurements. Additionally, the higher concentrations used in these experiments provide for greater certainty in the initial concentration of toluene compared to the extremely low concentrations required by ARAS measurements.

2. Experimental and modeling

The experiments reported here were performed behind reflected shock waves in a pressure-driven stainless steel shock tube facility that has been described previously [19,20]. Reflected shock conditions ranged from 1398 to 1782 K at total pressures around 1.5 bar. Test gas mixtures were made with 100, 200, and 400 ppm of toluene (99% purity) diluted in argon (99.999% purity) in a high-purity turbo-pumped stainless steel mixing tank with an internal stirring system. The toluene was cycled through several freeze-pump-thaw cycles prior to introduction into a mixing tank to avoid impurities from high volatility species. Mixtures were allowed to mix for at least 4 h prior to shock wave experiments to allow for complete mixing.

Benzyl radicals have strong broadband absorption in the ultraviolet from 245 to 275 nm [12,21] allowing detection using laser absorption at 266 nm, a technique recently developed in our laboratory [20]. Continuous-wave laser radiation was generated at 266 nm (1.5 mW) by the single pass of a focused, 5 W, 532 nm laser beam (frequency-doubled Nd:YVO_4) through an angle-tuned beta barium borate (β-BaB_2O_4, BBO) crystal. After generation, the harmonic (266 nm) was separated from the fundamental (532 nm) in a Pellin-Broca prism. The 266 nm laser beam was split into two components: one, ~1 mm in diameter, passing through the shock tube as a diagnostic beam (I), and one detected prior to absorption as a reference (I_0). Optical measurements were made at a location 2 cm from the endwall. The shock-heated gases were accessed through 0.75″ diameter flat wedged windows made of UV fused silica flush-mounted to the inner radius of the shock tube. The intensities of the reference and diagnostic beams were measured using amplified silicon photodiodes (Hamamatsu S1722-02, risetime < 0.5 μs, 4.1 mm diameter) and recorded on a digital oscilloscope.

The benzyl absorption cross-section at 266 nm has been measured in our laboratory by shock heating mixtures of benzyl iodide (50 and 100 ppm) dilute in argon to produce known, instantaneous, post-shock benzyl yields [20]. In these experiments the benzyl absorption cross-section was determined from the time-zero absorption of the immediate benzyl yield. Following the immediate benzyl yield the concentration of benzyl decays due to thermal decomposition of benzyl, yielding a C_7H_6 fragment of unknown structure and an H-atom:

$$C_6H_5CH_2 \rightarrow C_7H_6 + H \quad (3)$$

The benzyl fragment product shows non-negligible absorption at 266 nm that must be accounted for. The absorption cross-section of the benzyl fragment was determined by assuming complete one-to-one conversion of benzyl to fragments at long times after the absorption had decayed to a plateau. The 266 nm absorption cross-sections for the benzyl radical and the benzyl fragments was determined, from the benzyl iodide decomposition experiments, to be $\sigma_{\text{benzyl}}(266\text{ nm}) = 1.9\ (\pm 0.2) \times 10^{-17}\ \text{cm}^2\,\text{molecule}^{-1}$ and $\sigma_{\text{fragment}}(266\text{ nm}) = 3.4\ \ (\pm 0.5) \times 10^{-18}\ \text{cm}^2\,\text{molecule}^{-1}$, respectively [20]. Additionally, both the benzyl and the benzyl fragment absorption cross-sections showed no discernable temperature dependence across the experimental range of the benzyl iodide experiments (1430–1730 K) and therefore the cross-sections were treated as temperature-independent for the measurements reported here.

For the toluene decomposition experiments described here the absorption due to benzyl, benzyl fragments, and toluene must be accounted for. Therefore, the measured fractional absorption (I/I_0) is expressed, via Beer's law, in terms of the contribution to the absorbance by the three absorbing species

$$\begin{aligned} I/I_0 &= \exp(-\text{absorbance}) = \exp\left(-L\sum \sigma_i n_i\right) \\ &= \exp[-L(\sigma_{\text{benzyl}} n_{\text{benzyl}} \\ &\quad + \sigma_{\text{benzyl fragment}} n_{\text{benzyl fragment}} \\ &\quad + \sigma_{\text{toluene}} n_{\text{toluene}})] \end{aligned}$$

In this formulation I is the transmitted laser intensity, I_0 is the reference beam intensity, σ_i [$\text{cm}^2\,\text{molecule}^{-1}$] is the absorption cross-section of the individual absorbing species, n_i [molecules cm^{-3}] is the number density of the species, and L is the absorption path length (diameter of the shock tube, 14.13 cm).

The absorbance at 266 nm for an example toluene decomposition experiment is shown in Fig. 1. Prior to the passage of the incident shock wave, no absorption by toluene was detected at the low initial pressure, P_1. The passing of the incident shock wave causes the test gas to be compressed and heated, causing the toluene to absorb slightly (~0.4% absorbance at $t \approx -60$ μs in Fig. 1). The passage of the reflected shock wave causes a schlieren spike in the absorbance trace (density deflection) and the toluene absorbs at time-zero more strongly due to the increased density (~1% absorbance at time-zero in Fig. 1). The absorption cross-section for toluene was determined from this time-zero absorbance prior to toluene decomposition. The cross-section was determined to be $\sigma_{\text{toluene}}(266\text{ nm}) = 5.9\ (\pm 0.6) \times 10^{-19}\ \text{cm}^2\,\text{molecule}^{-1}$ with no discernable temperature-dependence over the range of temperatures examined in this study. After the passage of the reflected shock wave the more strongly absorbing benzyl radical is formed via reaction (1). Toluene is known to decompose via both reactions (1) and (2) at high-temperatures. Therefore, the benzyl absorbance profiles must be fit in terms of the overall decomposition rate coefficient, $k_1 + k_2$, and the branching ratio, $k_1/(k_1 + k_2)$. The parallel two-channel decomposition was fit in the standard manner: the early time rise was fit by adjusting the overall rate, $k_1 + k_2$, and the later time rolloff (peak amplitude of absorbance) was fit by adjusting the branching ratio, $k_1/(k_1 + k_2)$.

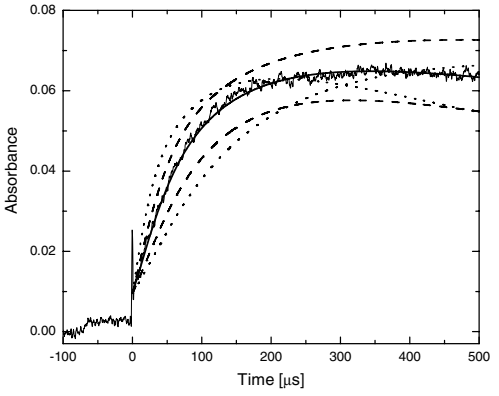

Fig. 1. Example 266 nm absorbance during toluene decomposition. Reflected shock conditions: 1593 K, 1.44 bar, 200 ppm toluene/Ar. Solid line, fit to data by adjusting overall decomposition rate, $k_1 + k_2$, and branching ratio, $k_1/(k_1 + k_2)$; dotted lines, variation of $k_1 + k_2 \pm 50\%$; dashed lines, variation of $k_1/(k_1 + k_2) \pm 30\%$.

The measured 266 nm absorbance, see Fig. 1 for an example, was fit by adjusting the overall decomposition rate and the branching ratio in a kinetic mechanism (see Table 1) developed primarily by Troe, Hippler, and co-workers [8,13,22–24] and by accounting for the contributions to the absorption due to benzyl, benzyl fragments, and toluene. Note that reverse reactions were included (for reactions written using the forward and backward arrow) using the thermochemical data of Burcat [25] and the given forward rate coefficients in Table 1. Reaction (−1), reverse of reaction (1), is significant under these conditions; however, recent improvements in the thermochemical data for benzyl [26] allow accurate calculation of the reaction (−1) rate coefficient based on the rate determination of the forward rate coefficient. In Fig. 1 the best fit to the example experimental trace is shown along with perturbations on the fit that result by varying the overall rate, $k_1 + k_2$, ±50% and the branching ratio, $k_1/(k_1 + k_2)$, ±30%. The contribution each of the three absorbing species has toward the total

Table 1
Reaction mechanism used for modeling toluene decomposition, rate coefficients in the form $k = AT^b \exp(-E_a/RT)$

	Reaction	A [cm, mol, s]	b	E_a [cal/mol]	Reference
(1)	$C_6H_5CH_3 \leftrightarrow C_6H_5CH_2 + H$ (1.5 bar)	2.09×10^{15}	0	87510	This study
(2)	$C_6H_5CH_3 \leftrightarrow C_6H_5 + CH_3$ (1.5 bar)	2.66×10^{16}	0	97880	This study
(3)	$C_6H_5CH_2 \rightarrow C_7H_6 + H$	8.20×10^{14}	0	80670	[20]
(−3)	$C_7H_6 + H \rightarrow C_6H_5CH_2$	1.00×10^{14}	0	0	[14]
(4)	$C_6H_5CH_3 + H \leftrightarrow C_6H_5CH_2 + H_2$	1.26×10^{15}	0	14818	[8]
	$C_6H_5 \leftrightarrow C_6H_4 + H$	8.00×10^{41}	−7.72	92210	[28]
	$C_6H_5 + H \leftrightarrow C_6H_6$	7.80×10^{13}	0	0	[29]
	$H + C_6H_5CH_3 \leftrightarrow CH_3 + C_6H_6$	5.78×10^{13}	0	8090	[30]
	$CH_3 + C_6H_5CH_3 \leftrightarrow C_6H_5CH_2 + CH_4$	3.16×10^{12}	0	0	[31]
	$C_6H_5 + C_6H_5CH_3 \leftrightarrow C_6H_6 + C_6H_5CH_2$	7.94×10^{13}	0	11940	[23]
	$C_6H_5CH_2 + C_6H_5CH_2 \rightarrow C_6H_5CH_2CH_2C_6H_5$	5.01×10^{12}	0	454	[22]
	$C_6H_5CH_2CH_2C_6H_5 \rightarrow C_6H_5CH_2 + C_6H_5CH_2$	7.94×10^{14}	0	59751	[22]
	$C_6H_5CH_2CH_2C_6H_5 \rightarrow C_6H_5CH_2CHC_6H_5 + H$	1.00×10^{16}	0	83660	[24]
	$C_6H_5CH_2CH_2C_6H_5 + H \rightarrow C_6H_5CH_2CHC_6H_5 + H_2$	3.16×10^{12}	0	0	[13]
	$C_6H_5CH_2CHC_6H_5 \rightarrow C_6H_5CHCHC_6H_5 + H$	7.94×10^{15}	0	51864	[13]

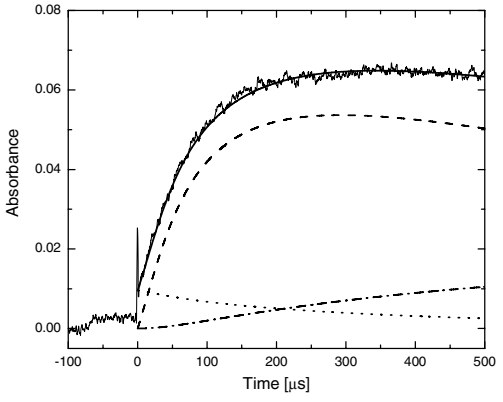

Fig. 2. Contribution to 266 nm absorbance. Contribution from benzyl (dashed line), from benzyl fragment (dashed–dotted line), and from toluene (dotted line), for example, experiment given in Fig. 1.

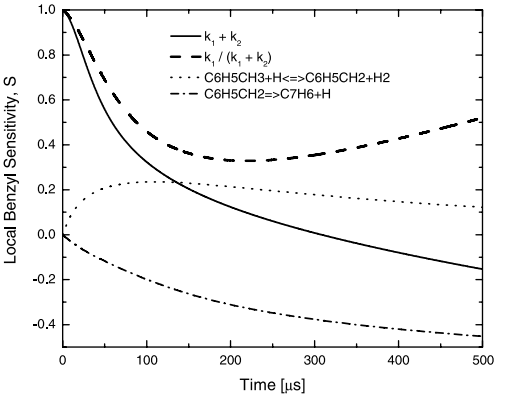

Fig. 3. Local sensitivity for benzyl concentration for conditions of experiment given in Fig. 1. $S = (dX_{benzyl}/dk_i)$ $(k_i/X_{benzyl,local})$, where k_i is the rate constant for reaction i and $X_{benzyl,local}$ is the benzyl ($C_6H_5CH_2$) mole fraction at time t.

signal is shown in Fig. 2. Note that the majority of the temporal behavior of the measured absorbance is dependent on the benzyl concentration; the two interfering species, toluene and the benzyl fragment, generate a slowly varying absorbance baseline. Absorbance due to other interfering species (C_6H_5, C_6H_6, C_6H_4, and $C_6H_5CH_2CH_2C_6H_5$) was considered but found to be negligible due to the smaller absorption cross-sections at 266 nm of these species and the small concentrations of these species present during these experiments. However, uncertainty in the interfering absorption was accounted for in the estimate of uncertainty in the resulting rate coefficient.

A benzyl sensitivity calculation for the conditions of Fig. 1 is shown in Fig. 3. The calculation shows strong sensitivity to the overall decomposition rate, $k_1 + k_2$, and the branching ratio, $k_1/(k_1 + k_2)$. The sensitivity of the overall rate and branching ratio show different temporal behavior allowing for the separation of the two parameters needed to fit both parameters with one experimental observable. The sensitivity calculation also shows unavoidable interference from fast secondary reactions:

$$C_6H_5CH_2 \rightarrow C_7H_6 + H \quad (4)$$

$$C_6H_5CH_3 + H \rightarrow C_6H_5CH_2 + H_2 \quad (5)$$

The rate coefficients for reactions (3) and (4) are well-known with uncertainties of ±25% and ±30%, respectively. Reaction (3) was part of a recent study carried out in our laboratory [20] and reaction (4) has been previously measured by Hippler and co-workers [8]. The sensitivity to these reactions is unavoidable and somewhat increases the uncertainty in the current rate determinations.

The rate coefficient results for toluene decomposition at 1.5 bar are given in Figs. 4 and 5 with

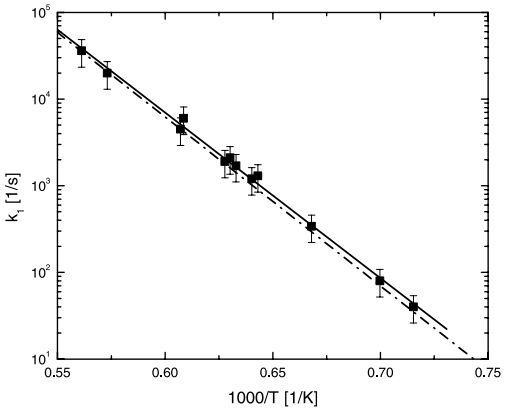

Fig. 4. Rate coefficient for $C_6H_5CH_3 \rightarrow C_6H_5CH_2 + H$, reaction (1). Filled squares with error bars, current experimental results (~1.5 bar); solid line, least-squares fit to current data; dash–dot line, Baulch et al. [27] IUPAC recommendation for $k_{\infty,1}$.

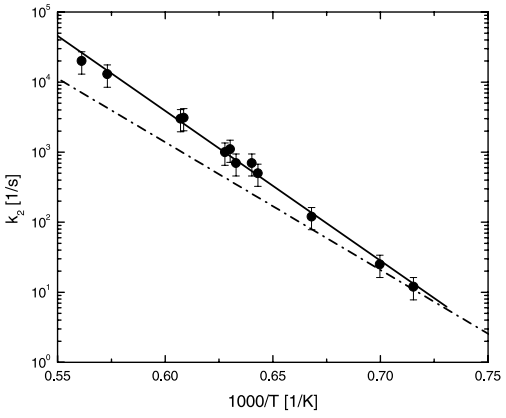

Fig. 5. Rate coefficient for $C_6H_5CH_3 \rightarrow C_6H_5 + CH_3$, reaction (2): filled circles with error bars, current experimental results (~1.5 bar); solid line, least-squares fit to current data; dash–dot line, Baulch et al. [27] IUPAC recommendation for $k_{\infty,2}$.

least-squares fit. Expressions for the rate coefficients for reactions (1) and (2) at 1.5 bar given by the least-squares fit are

$$k_1(T) = 2.09 \times 10^{15} \exp(-87510\ [\text{cal/mol}]/RT)[\text{s}^{-1}] \quad (6)$$

$$k_2(T) = 2.66 \times 10^{16} \exp(-97880\ [\text{cal/mol}]/RT)[\text{s}^{-1}] \quad (7)$$

where the RMS experimental scatter about the fits is ±13% and ±17% for k_1 and k_2, respectively. The rate coefficient determinations for reactions (1) and (2) are tabulated in Table 2. The primary contributions to uncertainties in the rate coefficients are uncertainties in: temperature, absorption cross-sections, fitting the data to computed profiles, and interfering chemistry. These uncertainties give overall uncertainties in k_1 and k_2 of ±35%, and ±35%, respectively. Based on the falloff calculations of Eng et al. [14] it is expected that the current rate coefficient results are approximately a factor of 2 from the high-pressure limit at the highest temperatures of this study (1780 K) and approximately 20–30% from the high-pressure limit at 1400 K.

3. Discussion

The results of the current toluene decomposition study, in terms of the overall decomposition rate coefficient and the branching ratio, are compared to previous studies in Figs. 6 and 7. The current findings for the overall decomposition rate coefficient agree, with deviation of less than 30%, with previous results of Eng et al. [14], Braun-Unkhoff et al. [15], and Luther et al. [18]. However, the results for the overall decomposition rate coefficient of Pammidimukkala et al. [7] and Rao and Skinner [16] are significantly lower than the current findings (Fig. 6). The results of the current study for the branching ratio are in good agreement with the previous findings of Eng et al. [14] and Luther et al. [18]. However, the results of the current study are in disagreement with the results of Pammidimukkala et al. [7], Rao and Skinner [16], and Braun-Unkhoff et al. [15]. The current data set and the recent H-atom ARAS experiments of Eng et al. [14] clearly show that the toluene decomposition channel leading to benzyl, reaction (1), is dominant over the channel leading to phenyl, reaction (2). On these grounds the low branching ratios given by the earlier studies of Pammidimukkala et al. [7] and Rao and Skinner [16] are probably erroneous. Additionally the relatively low uncertainties of the current results and the excellent agreement with the low concentration (high kinetic isolation) H-atom ARAS results of Eng et al. [14] lends confidence to the results presented here. The consensus between the current study, the H-atom ARAS study of Eng et al. [14], and the laser excitation study of Luther et al. [18] is of note because all three rate determinations were made using different techniques. This consensus provides sufficient basis for future models of aromatic oxidation to use the rate coefficients provided here, particularly, in light of the large deviations in the decomposition branching ratios used in current models [1–6] and the importance of the branching ratio in describing the overall reactivity of toluene (reaction (1) produces a relatively non-reactive, resonantly stable benzyl radical and reaction (2) produces a reactive phenyl radical).

Table 2
Summary of experimental results for toluene decomposition

Mixture	Temperature [K]	Pressure [bar]	k_1 [1/s]	k_2 [1/s]
100 ppm toluene/Ar	1555	1.54	1.3×10^{3}	5.0×10^{2}
	1587	1.54	2.1×10^{3}	1.1×10^{3}
	1643	1.50	6.0×10^{3}	3.1×10^{3}
200 ppm toluene/Ar	1497	1.56	3.4×10^{2}	1.2×10^{2}
	1580	1.49	1.7×10^{3}	7.0×10^{2}
	1593	1.44	1.9×10^{3}	1.0×10^{3}
	1782	1.42	3.6×10^{4}	2.0×10^{4}
400 ppm toluene/Ar	1398	1.48	4.0×10^{1}	1.2×10^{1}
	1429	1.50	8.0×10^{1}	2.5×10^{1}
	1562	1.51	1.2×10^{3}	7.0×10^{2}
	1647	1.41	4.5×10^{3}	3.0×10^{3}
	1745	1.46	2.0×10^{4}	1.3×10^{4}

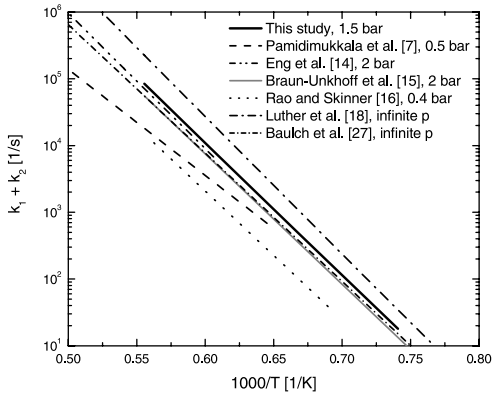

Fig. 6. Comparison with previous data for the toluene overall decomposition rate coefficient $k_1 + k_2$.

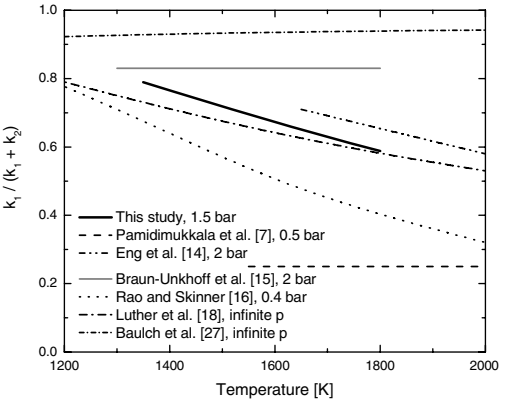

Fig. 7. Comparison with previous data for the toluene decomposition branching ratio $k_1/(k_1 + k_2)$.

A comparison of the toluene decomposition results with the most recent International Union of Pure and Applied Chemistry (IUPAC) recommendations (Baulch et al. [27]) is also made in Figs. 4–7. The IUPAC recommendation for the toluene → benzyl + H channel, k_1, shows good agreement. However, the recommendation for the toluene → phenyl + CH_3 channel, k_2, shows large disagreement. The IUPAC recommendation is based on the results of Pammidimukkala et al. [7] and has far too low an activation energy and A-factor in comparison to the current study and previous studies. The experiments of Pammidimukkala et al. [7] were complicated by the high initial concentrations of toluene used (0.5–4%) and enhanced falloff effects due to the low-pressures the experiments were performed under (0.2–0.5 bar). The disagreement for k_2 between the IUPAC recommendation and the findings of this work result in disagreement in the magnitude of the branching ratio and the temperature-dependence, Fig. 7.

4. Conclusions

The two-channel decomposition of toluene has been studied at temperatures ranging from 1400 to 1780 K and at total pressures of 1.5 bar using shock wave heating and ultraviolet laser absorption of benzyl at 266 nm. The temporal behavior of the 266 nm absorption traces allowed determination of the overall toluene decomposition rate coefficient and branching ratio. The low concentrations used (100, 200, and 400 ppm toluene/Ar) and the high levels of signal-to-noise provided by the laser absorption technique allowed for the determination of k_1 and k_2 with an uncertainty of ±35%. The rate coefficient results are in excellent agreement with the previous rate determinations made by Luther et al. [18] and Eng et al. [14].

Acknowledgments

This work was supported by the US Department of Energy, Chemical Sciences Division, Office of Basic Energy Sciences, with Dr. Frank Tully as con-

tract monitor and the US Department of Energy Consortium on HCCI Engine Research.

References

[1] R. Bounaceur, I. Da Costa, R. Fournet, F. Billaud, F. Battin-Leclerc, *Int. J. Chem. Kinet.* 37 (2005) 25–49.
[2] S.D. Klotz, K. Brezinsky, I. Glassman, *Int. J. Chem. Kinet.* 27 (1998) 337–344.
[3] P. Dagaut, G. Pengloan, A. Ristori, *Phys. Chem. Chem. Phys.* 4 (2002) 1846–1854.
[4] R.P. Lindstedt, L.Q. Maurice, *Combust. Sci. Technol.* 120 (1996) 119–167.
[5] W.J. Pitz, R. Seiser, J.W. Bozzelli, et al., in: *Proceedings of the 2nd Joint Meeting of the US. Sections of the Combustion Institute*, 2001.
[6] Z.M. Djurisic, A.V. Joshi, H. Wang, in: *Proceedings of the 2nd Joint Meeting of the US Sections of the Combustion Institute*, 2001.
[7] K.M. Pamidimukkala, R.D. Kern, M.R. Patel, H.C. Wei, J.H. Kiefer, *J. Phys. Chem.* 91 (1987) 2148–2154.
[8] H. Hippler, C. Reihs, J. Troe, *Z. Phys. Chem. (Neue Folge)* 167 (1990) 1–16.
[9] W. Müller-Markgraf, J. Troe, *Proc. Combust. Inst.* 21 (1986) 815–824.
[10] D.C. Astholz, J. Troe, *J. Chem. Soc. Faraday Trans. 2* 78 (1982) 1413–1421.
[11] D.C. Astholz, J. Durant, J. Troe, *Proc. Combust. Inst.* 18 (1981) 885–892.
[12] W. Müller-Markgraf, J. Troe, *J. Phys. Chem.* 92 (1988) 4899–4905.
[13] L.D. Brouwer, W. Müller-Markgraf, J. Troe, *J. Phys. Chem.* 92 (1988) 4905–4914.
[14] R.A. Eng, A. Gebert, E. Goos, H. Hippler, C. Kachiani, *Phys. Chem. Chem. Phys.* 4 (2002) 3989–3996.
[15] M. Braun-Unkhoff, P. Frank, Th. Just, *Proc. Combust. Inst.* 22 (1988) 1053–1061.
[16] V.S. Rao, G.B. Skinner, *J. Phys. Chem.* 93 (1989) 1864–1869.
[17] U. Brand, H. Hippler, L. Lindemann, J. Troe, *J. Phys. Chem.* 94 (1990) 6305–6316.
[18] K. Luther, J. Troe, K.-M. Weitzel, *J. Phys. Chem.* 94 (1990) 6316–6320.
[19] M.A. Oehlschlaeger, D.F. Davidson, R.K. Hanson, *J. Phys. Chem. A* 108 (2004) 4247–4253.
[20] M.A. Oehlschlaeger, D.F. Davidson, R.K. Hanson, *J. Phys. Chem. A* 110 (2006) 6649–6653.
[21] N. Ikeda, N. Nakashima, K. Yoshihara, *J. Phys. Chem.* 88 (1984) 5803–5806.
[22] H. Hippler, J. Troe, *J. Phys. Chem.* 94 (1990) 3803–3806.
[23] E. Heckmann, H. Hippler, J. Troe, *Proc. Combust. Inst.* 26 (1996) 543–550.
[24] H. Hippler, C. Reihs, J. Troe, *J. Proc. Combust. Inst.* 23 (1990) 37–43.
[25] A. Burcat, B. Ruscic, *Ideal Gas Thermochemical Database with updates from Active Thermochemical Tables*. Available at <ftp://ftp.technion.ac.il/pub/supported/aetdd/thermodynamics/>, 2006; mirrored at <http://garfield.chem.elte.hu/burcat/burcat.html/>, 2006.
[26] S. Song, D.M. Golden, R.K. Hanson, C.T. Bowman, *J. Phys. Chem. A* 106 (2002) 6094–6098.
[27] D.L. Baulch, C.T. Bowman, C.J. Cobos, et al., *J. Phys. Chem. Ref. Data* 34 (2005) 757–1397.
[28] L.K. Madden, L.V. Moskaleva, S. Kristyan, M.C. Lin, *J. Phys. Chem. A* 101 (1997) 6790–6797.
[29] D.L. Baulch, C.J. Cobos, R.A. Cox, et al., *J. Phys. Chem. Ref. Data* 21 (1992) 411–734.
[30] D.L. Baulch, C.J. Cobos, R.A. Cox, et al., *J. Phys. Chem. Ref. Data* 23 (1994) 847–1033.
[31] T.A. Litzinger, K. Brezinsky, I. Glassman, *Combust. Flame* 63 (1986) 251–267.

Comments

John Kiefer, UIC, USA. You are making a lot of C_6species (C_6H_5, C_6H_4)…. What is the absorbance of these species?

Reply. The C_6 species (C_6H_6, C_6H_5, C_6H_4, etc.) have peak absorption at wavelengths of 240 nm or less and decline toward the red [1–3]. The strongest C_6 absorber is phenyl (C_6H_5) which has an absorption cross-section of $\sim 2 \times 10^{-17}$ cm^3 molecule^{-1} at its 240 nm peak and a cross-section of $\sim 5 \times 10^{-18}$ cm^3 molecule^{-1}at 266 nm [2]. Fortunately, in these experiments the peak concentration of C_6H_5 is very small ($\sim$2 ppm), due to fast C_6H_5 decomposition and reaction with H atoms and toluene. Therefore, the C_6H_5 absorption contribution can be neglected (we estimate that the absorbance due to C_6H_5 is $\sim$0.001). The stable C_6 species formed at higher concentrations in these experiments are expected to have much smaller absorption cross-sections (10^{-20}–10^{-19} cm^3 molecules^{-1}) in comparison to the phenyl radical, as is typical of stable species in comparison to radicals of similar structure. For example, benzene has a cross-section of $\sim 2 \times 10^{-20}$ cm^3 molecule^{-1}at 266 nm.

References

[1] E.E. Rennie, C.A.F. Johnson, J.E. Parker, D.M.P. Holland, D.A. Shaw, M.A. Hayes, *Chem. Phys.* 229 (1998) 107–123.
[2] T.J. Wallington, H. Egsgaard, O.J. Nielsen, J. Platz, J. Sehested, T. Stein, *Chem. Phys. Lett.* 290 (1998) 363–370.
[3] J.G.G. Simon, N. Münzel, A. Schweig, *Chem. Phys. Lett.* 170 (1990) 187–192.

●

Joe Michael, Argonne National Laboratory, USA. What absolute number density do you obtain in your profiles? The reason I ask is that atomic H atom ARAS can be carried out at 10–50 times more sensitivity, thereby eliminating secondary reactions and absorptions that you have to take into account in your analysis.

Marina Braun-Unkhoff, DLR Stuttgart, Germany. Several years ago we carried out several shock tube

studies on the pyrolysis of toluene, benzyl and phenyl radicals, as well as on the methyl disproportion reactions ($2CH_3 \rightarrow C_2H_5 + H \rightarrow C_2H_4 + H$). We were able to use very, very small initial concentrations as we used H-ARAS as a very sensitive detection technique. Thus, the influence of secondary reactions was considerably reduced and the rate coefficients reported were derived very sensitive including the branching ratio we reported. As you are using much higher initial concentrations, I wonder what might be the influence of boundary reactions on your reported branching ratio.

Reply. The minimum detectable benzyl concentration is approximately 4×10^{12} molecules cm^{-3} in these experiments and the peak concentration in the experiment shown in Fig. 1 is 2×10^{14} molecules cm^{-3}. Yes, the minimum detectable concentration is approximately an order-of-magnitude greater than that which can be detected with H atom ARAS, and our initial concentrations are significantly greater. However, the *absorbance* signal-to-noise ratio of the laser absorption technique used in these experiments is approximately an order-of-magnitude greater than that which can be achieved using ARAS. The high *absorbance* S/N allows precise and easy fitting of modeling calculations to the data traces and therefore provides rate coefficient determinations with minimal scatter (13% and 17% RMS). Additionally, the rate coefficients have uncertainty (estimated to be ±35%) due almost exclusively to uncertainties in the secondary chemistry rather than uncertainty due to absorbance noise. In contrast, H atom ARAS measurements typically provide rate coefficients with uncertainty dominated by absorbance noise and with much greater scatter due to the order-of-magnitude poorer *absorbance* S/N of ARAS in comparison to laser absorption. For example, the experimental scatter (not uncertainty) in the ARAS measurements of references Eng et al. ([14] in paper) and Braun-Unkhoff et al. ([15] in paper) is ±30% and ±50%, respectively (estimated from published figures within those references). Therefore, the experimental uncertainty is at least ±30% and ±50%, for those respective studies, and presumably somewhat greater due to other systematic uncertainties that do not manifest as scatter in the rate results. While ARAS provides an order-of-magnitude better sensitivity, it also has the unfortunate characteristics of being quite noisy. On the other hand, laser absorption provides much greater *absorbance* S/N but with a higher detectable concentration limit requiring, in some cases such as that encountered in this work, knowledge of secondary chemistry. These are clear tradeoffs between the two diagnostic techniques. Most importantly, the higher concentration measurements we present here and lower concentration ARAS measurements of Eng et al. ([14]in paper) agree, indicating that the rate parameters for the important secondary reactions are presumably fairly accurate.

•

Ken Brezinsky, University of Illinois at Chicago, USA. Recently we published an extensive analysis of the toluene decomposition branching ratio [1]. In the study we found it necessary to carefully select an appropriate heat of formation for the phenyl and benzyl radicals in order to simulate our high pressure shock tube results. Have you examined the effect on your branching ratios of the choice of these heats of formation?

Reference

[1] K. Brezinsky et al., *J. Phys. Chem. A.* 110 (2006) 9388–9399.

Reply. The current rate results and branching ratio are sensitive to the heat of formation of the benzyl radical due to the relatively fast k_{-1} reverse reaction and the large concentrations of benzyl present. However, our results are not strongly sensitive to the phenyl heat of formation due to the somewhat slower k_{-2} in comparison to k_{-1} and the smaller phenyl concentrations relative to benzyl (due to fast C_6H_5 decomposition and fast reaction with H atoms and toluene). We used a value of $\Delta_f H^o_{298}(\text{benzyl}) = 49.7$ kcal mol^{-1} for the heat of formation of benzyl, which has an estimated uncertainty of ±0.5 kcal mol^{-1} ([25] in paper). Yes, the uncertainty in the benzyl heat of formation does influence the branching ratio; the uncertainty was accounted for in the estimated uncertainty in the rate coefficients, ±35% in k_1 and k_2. At the pressures encountered in your high-pressure shock tube experiments the reverse reactions k_{-1} and k_{-2} should be even more important and these heats of formation will influence the branching ratio to a greater degree. We note that you use a heat of formation for benzyl of 51.1 kcal mol^{-1} in the work you cite above. This value seems high in light of the number of experiments that have suggested a somewhat lower value: $\Delta_f H^o_{298} = 50.3$ kcal mol^{-1}, Hippler and Troe [1];$\Delta_f H^o_{298} = 48.5$ kcal mol^{-1}, Walker and Tsang [2]; $\Delta_f H^o_{298} = 49.7$ kcal mol^{-1}, Ellison et al. [3]; $\Delta_f H^o_{298} = 50.2$ kcal mol^{-1}, Song et al. [4]; and $\Delta_f H^o_{298} = 49.7$ kcal mol^{-1}, Muralha et al. [5].

References

[1] H. Hippler, J. Troe, *J. Phys. Chem.* 94 (1990) 3803–3806.
[2] J.A. Walker, W. Tsang, *J. Phys. Chem.* 94 (1990) 3324–3327.
[3] G.B. Ellison, G.E. Davico, V.M. Bierbaum, C.H. DePuy, *Int. J. Mass Spectrom. Ion Process.* 156 (1996) 109–131.
[4] S. Song, D.M. Golden, R.K. Hanson, C.T. Bowman, *J. Phys. Chem. A* 106 (2002) 6094–6098.
[5] V.S.F. Muralha, R.M. Borges dos Santos, J.A.M. Simoes, *J. Phys. Chem. A* 108 (2004) 936–942.

•

Tsang Wing, NIST, USA. These reactions should have pressure dependence. This is especially the case for the branching ratios. Thus, comparisons with literature must therefore take pressure effects into consider-

ation. Please comment on how you have dealt with these effects.

Reply. In the temperature range of these experiments (1400–1780 K) the rate results are near the high-pressure limit. According to the calculation of Klippenstein et al. [1], k_1 and k_2 are within a few percent of the high-pressure limit at 1400 K and are within 40% of the high-pressure limit at 1780 K. At 1780 K we measure a branching ratio, $k_1/(k_1 + k_2)$, of 0.59 at 1.5 bar. Klippenstein et al. report a branching ratio of 0.62 at 1 bar and 0.59 at infinite pressure, indicating the pressure dependence of the branching ratio is small at the conditions of these experiments. The level of falloff in the rate coefficients and branching ratio is comparable in magnitude to the experimental uncertainties (35% in k_1 and k_2) and comparable to the level of scatter in the rate determinations (~15% for these measurements and 30–50% for previous studies). Therefore, direct comparisons of rate parameters, particularly the branching ratio, at pressures in excess of ~1 bar and at temperatures below ~1800 K can be done without accounting for pressure dependence, as is shown in Figs. 6 and 7. However, we should note that the some of the disagreement shown in Fig. 6 between the current study and Pamidimukkala et al. ([7] in paper) (0.5 bar) and Rao and Skinner ([16] in paper) (0.4 bar) is do to pressure falloff effects in their experiments.

Reference

[1] S.J. Klippenstein, L.B. Harding, Y. Georgievskii, *Proc. Combust. Inst.* 31 (2007) 221–229.

•

Jürgen Troe, University of Göttingen, Germany. The branching ratio is a function of temperature and pressure. Its modeling requires knowledge of the E- and T-dependencies of the specific rate constants k (E,T) of both channels in addition to information on every transfer. All these qualities have been determined experimentally by photo-excitation experiments [1] which are very accurate and uncontaminated by secondary reactions. Therefore, modeling of the properties of the branching ratio based on these data would give the most complete and most accurate results. It is very satisfactory to see that the present thermal experiments come close to the modeling results based on photo-excitation data.

Reference

[1] K. Luther, J. Troe, K.-M. Weitzel, *J. Phys. Chem.* 94 (1990) 6316.

Reply. Thank you for the comment.

•

M.C. Lin, Emory University, USA. This is very nice work. I would like to point out that our old [1] and new [2] kinetic data for the combination of CH_3 with C_6H_5 measured for 300–1000 K converted to that for the dissociation of toluene covering the 300–2000 K temperature range using Frenkel's [3] thermo-chemistry data for CH_3, C_6H_5 and $C_6H_5CH_3$ gives rise to $k_2 = (1.84 \pm 0.11) \times 1D^{17} e^{-(52070 \pm 30)/T} s^{-1}$. The combination of our k_2 with your value obtained by shock-heating leads to $k_2 = (2.37 \pm 0.13) \times 10^{17} e^{-(52{,}180 \pm 26)/T} s^{-1}$. Apparently your data and ours for $CH_3 + C_6H_5$ correlate quite well.

References

[1] I.V. Tokmakav, J. Park, S. Gheyas, M.C. Lin, *J. Phys. Chem. A.* 103 (1999) 3636–3645.
[2] J. Park, M.C. Lin, unpublished data.
[3] M.L. Frenkel, *Thermodynamics of Organic Compounds in the Gas State*, Thermodynamics Research Center, College Station, Texas, 1994.

Reply. Thank you for the comment.